AIAA JOURNAL
Vol. 54, No. 2, February 2016

Technical Notes

TECHNICAL NOTES are short manuscripts describing new developments or important results of a preliminary nature. These Notes should not exceed 2500 words (where a figure or table counts as 200 words). Following informal review by the Editors, they may be published within a few months of the date of receipt. Style requirements are the same as for regular contributions (see inside back cover).

Nonlinearity of Apparent Mass for Multielement Bodies

Kenneth O. Granlund* and Michael V. Ol†
U.S. Air Force Research Laboratory, Wright–Patterson Air Force Base, Ohio 45433
and
Luis P. Bernal‡
University of Michigan, Ann Arbor, Michigan 48109

DOI: 10.2514/1.J054214

Nomenclature

b	=	plate span equal to $4c$ (450 mm)
c	=	plate chord (75 mm)
d	=	plate spacing normalized by chord c
$E(m)$	=	complete elliptic integral of the second kind ($\int_0^{\pi/2}\sqrt{1-m^2\sin^2\theta}\,\mathrm{d}\theta$)
$F(m)$	=	complete elliptic integral of the first kind ($\int_0^{\pi/2}\mathrm{d}\theta/\sqrt{1-m^2\sin^2\theta}$)
F_a	=	amplitude of the force per unit span, N/m
$F_p(t)$	=	theoretical force acting on the plate, N
F'_p	=	force per unit span, N/m
h_0	=	oscillation amplitude normalized by chord c
t	=	time, s
u	=	plate speed, m/s
ρ	=	fluid density (1000 kg/m^3)

I. Introduction

CLASSICAL [1–5], and recent [6–12] expositions of the aerodynamic force history of unsteady incompressible problems segregate the forces into those due to the relative acceleration between the body immersed in a fluid, and everything else. Loads due to acceleration are referred to as inertial, noncirculatory, or apparent (or added) mass, since their cause is imputed to acceleration of a volume of bulk fluid of some density (hence, inertia) to causes other than circulation or to what mathematically looks like a slug of fluid moving with the accelerating body, respectively. The "everything else" lumps together forces due to bound or shed circulation, forces due to flow separation, and viscous traction. Ultimately, all aerodynamic loads are from integration of pressure distribution and viscous traction, so the distinction into circulatory and noncirculatory loads is somewhat artificial. However, it is a useful artifice because the noncirculatory loads are asserted to be independent of geometric details, such as sharp trailing edges supporting a Kutta condition or dynamic conditions such as Reynolds number. Further, one seeks to understand how unsteady a given unsteady problem really is, and this can be beheld from the ratio of circulatory to noncirculatory forces. If circulatory and noncirculatory force histories can be superimposed, this supports an argument for linear superposition, and hence for linearity. This would be particularly curious if the noncirculatory forces are the same in attached and in separated flows: for example, for a flat plate with strong vortex shedding from its edges and one without.

A simple classical unsteady incompressible problem is that of a thin, rigid, flat plate oscillating harmonically in the direction normal to its chord. The force per unit span is

$$F'_p = -\frac{\rho\pi c^2}{4}\frac{\mathrm{d}u}{\mathrm{d}t} \tag{1}$$

where u is the plate speed [13,14]. Thus, the constant of the force proportional to acceleration of a flat-plate body is equivalent to the mass of a circle of fluid encompassing the chord. Of course, the plate's motion produces an unsteady pressure field propagating everywhere in the fluid, with intensity decreasing away from the plate. That the force happens to be equal to that of an accelerating cylindrical mass of fluid around the plate is a convenient heuristic, and it is not an essential description of nature. But, it has emerged as an appealing technical term, and we follow such treatment here.

In the present work, we consider a flat plate spanning the width of the flow facility in a two-dimensional configuration. The theoretical force amplitude on a plate with span b and chord c, oscillated sinusoidally at an amplitude h_0c with frequency f, is

$$F_a(t) = -\frac{\rho\pi bc^2}{4}\frac{\mathrm{d}u}{\mathrm{d}t} = \rho\pi^3 bc^3 h_0 f^2\,\sin(2\pi f t) \tag{2}$$

The amplitude of the force per unit span F_a is normalized by the apparent mass of two single plates, such as the force amplitude being proportional to the oscillation frequency squared:

$$F_a = \max(F(t))/\rho\pi^3 bc^3 h_0 \tag{3}$$

In unsteady fluid mechanics force models, the fluid acceleratory term is derived from integrating the velocity potential in all of the fluid surrounding the body, assuming potential flow. High-rate large excursion motions produce massive separation and palpably violate the potential flow assumption. For cases such as pitching and plunging airfoils, one finds unsteady potential-flow models to be remarkably successful, regardless of motion frequency and up to motion amplitudes of an appreciable fraction of the airfoil chord. Granlund et al. [10] observed independence of a circulatory force from variations in the noncirculatory force for a plate pitching from 0 to 90 deg at the onset of the motion. We examine to what extent a similar success of theoretical models, with assumptions belied by observed reality, nevertheless yield predictions fitting the observed data. The approach is to vary the reduced frequency, the interplate gap, and the amplitude of motion, examining the near-plate flowfield with

Presented as Paper 2014-2882 at the 32nd AIAA Applied Aerodynamics Conference, Atlanta, GA, 16–20 June 2014; received 22 January 2015; revision received 26 July 2015; accepted for publication 4 September 2015; published online 15 December 2015.

*Aerospace Systems Directorate; kenneth.granlund@gmail.com. Senior Member AIAA.
†Aerospace Systems Directorate. Associate Fellow AIAA.
‡Department of Aerospace Engineering. Senior Member AIAA.

visualization by dye injection. Quantitatively, one compares measured vs theoretical forces. Qualitatively strong and persistent ejection of flow structures from the flap gap (between the plates or from the outboard edge) suggests that circulatory effects are nontrivial, and vice versa.

One immediately asks the following regarding linear superposition: "In the simplest such case, suppose that we have two plates adjacent to each other, some distance apart. Can the aforementioned solution for one plate be superimposed to that of the second for a combined solution?" The immediate answer is no. Consider the schematic in Fig. 1 where two plates are positioned far apart on the same chord line. Acceleration of one plate normal to the chord induces an acceleration of the surrounding fluid. Since the plates are far apart, the fluid acceleration of one has a minimal effect on the other, and vice versa; thus, the total force by both plates is the sum of the individual added mass multiplied by the acceleration.

If both plates are joined together, producing a $2c$ chord plate, the pressure field from an acceleration of the plate now produces an equivalent added mass of twice that of the individual plates together, since the constant in Eq. (1) is dependent on the chord squared. For the intermediate case of where the two plates are separated, but in close proximity to each other, the acceleration of fluid from one plate should now affect the other and the resulting equivalent added mass should be somewhere in between the two aforementioned extrema. The question is how the combined added mass as a function of chord separation looks like and whether it is affected by fluid viscosity, as the potential flow derivation is inviscid.

The analytical solution to two parallel plates was given by Sedov [13] and is shown in Eq. (4):

$$F_{\text{Sedov}} = -2\left(\frac{\rho\pi c^2}{4}\right)\frac{\partial u}{\partial t}2(1+d)^2\left(1-\frac{E(m)}{F(m)}\right), \quad m^2 = \frac{1}{(1+d)^2} \tag{4}$$

Here, in the limit of $d \to \infty$, the apparent mass approaches that of two single plates with c, and for $d \to 0$, it is $2c$.

II. Experimental Setup

Experiments were conducted at the U.S. Air Force Research Laboratory Horizontal Free-Surface Water Tunnel. The tunnel is fitted with a three-degree-of-freedom electric motion rig, controlled via a Galil DMC-4040 motion controller from preprogrammed scripts achieving less than 0.1 mm linear and less than 0.2 deg angular position errors. Two vertical linear motors move the test article linearly normal to the test section freestream direction (that is, in plunge).

Two carbon-fiber flat plates with 75 mm chord, 3 mm thickness, and 0.45 m span are positioned coplanar, with a coupler piece connecting to the load cell, shown in Fig. 1. The gap between the plate tips and the test section sidewalls is ≈1 mm. Chordwise spacing between the plates is taken as $0.05c$, $0.1c$, $0.2c$, and $0.5c$ by mounting the respective coupler piece. A case of a single plate of chord $2c$ serves as the baseline. The sinusoidal amplitude of the oscillation of the plates is varied as $0.01 < h_0 < 0.05$. Motions are also limited by motor maximum acceleration, setting an upper limit of product of frequency and amplitude.

According to Brennen [14], the proximity of a free surface to an accelerating body, which is less than four times the body dimension, will cause an increase in apparent mass with acceleration of the fluid. A distance between a free surface and a body of less than the body dimension will cause a decrease in apparent mass. Since the plates are oscillated at the centerline of the test section with exactly four chords to either the test section bottom wall and the free surface, it is expected that any boundary effects are minimized.

We first characterize the imposed kinematics, since the theoretical model assumes a perfect sinusoid. Figure 2 shows the linear vertical motor position and acceleration (A is front and B is rear in the top of Fig. 1) normalized to one. Both sets of curves show that acceleration is followed accurately and to the same magnitude as the prescribed motion. The low-frequency motion has a slight jitter at the acceleration peaks, which is attenuated to below observable level as the frequency is increased. Overall, though, there is no evidence of deviation from the prescribed motion that can cause unexpected results from acceleration of the flat plates in fluid.

Flow visualization is used as a qualitative surrogate for tracking vorticity, and thereby circulatory effects. Rhodamine 6G, illuminated by an approximately 2-mm-thick Nd:YLF laser light sheet pulsed at 100 Hz, is injected to the interplate gap and at the outboard edge of one of the plates, via 0.5-mm-diam tubes at the 3/4-span of the plate.

Force measurements were made with an ATI Nano25 IP68 six-component balance, sampled at 1 kHz and low-pass filtered at 34 Hz in the hardware, and then at 50 times the motion frequency using a fourth-order Chebyshev II low-pass filter in MATLAB. The data were synchronized externally via a trigger pulse from the DMC-4040 motion controller. All motions were repeated for 50 cycles, with the first three were not included in averaging.

Results from a mechanical strike test by tapping the plate with a metal rod and recording the frequency reveal that the eigenfrequency is 15.5 Hz, which is well above the highest forced oscillation frequency of 9 Hz.

In Fig. 3, the linearity in the dynamic response of the load cell is tested by oscillating a 0.468 kg steel disk attached to the load cell in air to simulate the apparent mass of a plate in water. The force signal amplitude is normalized by the mass times the acceleration to produce a linear relationship with the frequency squared.

An additional effect we have to consider is that the entire span of the plate does not exhibit uniform motion but, instead, has slight aeroelastic flutter. High-speed photogrammetry of the plate tip is

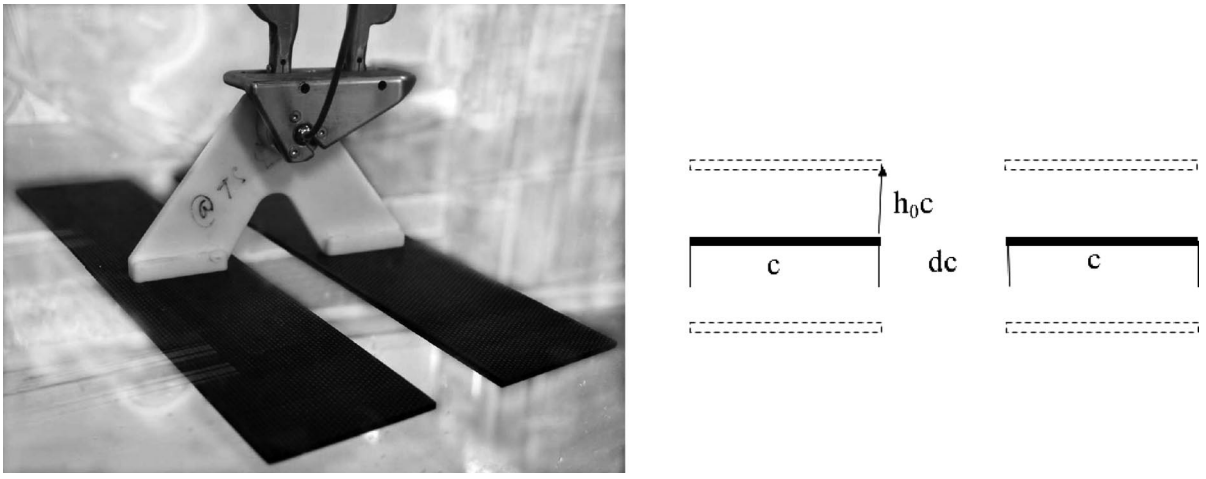

Fig. 1 Two wall-to-wall carbon-fiber flat plates mounted horizontally in the test section (left) and a schematic of the setup with a definition of variables (right).

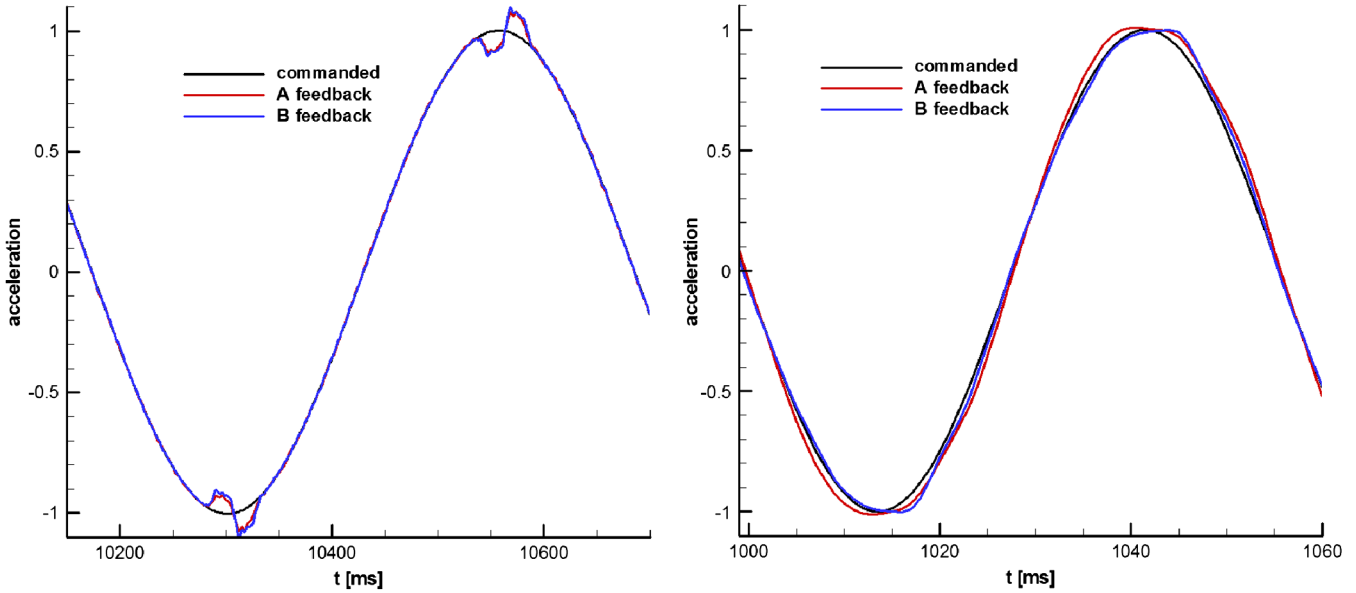

Fig. 2 Typical motion acceleration kinematics normalized by maximum value: 1 Hz, 0.05c (left) and 9 Hz, 0.01c (right). A and B are front and rear plunge rods visible in the top of Fig. 1.

performed with a PCO DiMax at 500 frames per second. A forced oscillation motion of 0.02c amplitude and 9 Hz reveals a tip deflection less than 110% of the forcing amplitude. To investigate this small aeroelastic phenomenon on the error in measurement of the apparent mass, we treat the plate as a cantilevered beam, clamped at the centerline, with a uniformly distributed load in Fig. 4. The deflection $\delta h_0 c$ at a spanwise location x is given by

$$\delta h_0 c = \frac{w}{24EI}(x^4 - 4(b/2)^3 x + 3(b/2)^4) \tag{5}$$

and the maximum defection at the tip $[x = (b/2)]$ is from photogrammetry:

$$\delta h_0 c|_{\max} = \frac{w(b/2)^4}{8EI} = 0.1 h_0 c \tag{6}$$

Since the apparent mass is proportional to the plate amplitude, we use the average aeroelastic deflection of the plate as the additional apparent mass:

$$\delta h_{0,\text{avg}} = \frac{1}{b/2}\frac{w}{24EI}\int_0^{b/2} x^4 - 4(b/2)^3 x + 3(b/2)^4 \, dx$$
$$= \frac{1}{3}\frac{w(b/2)^4}{8EI}\frac{4}{5} = 0.0266 h_0 c \tag{7}$$

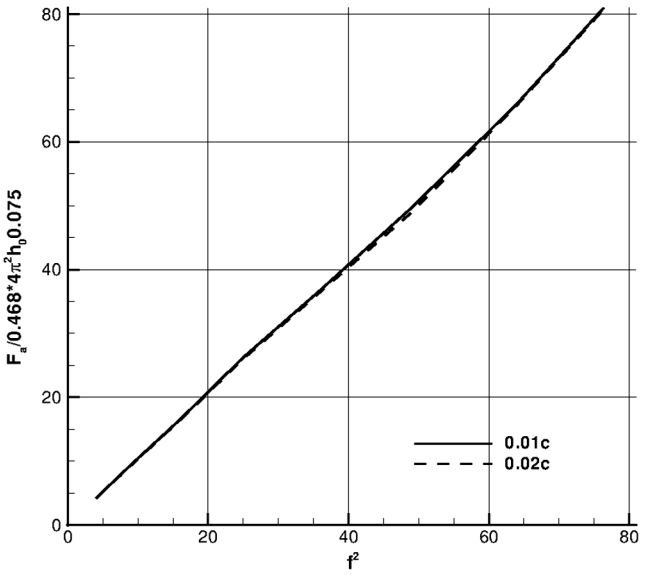

Fig. 3 Sinusoidal oscillation of 0.468 kg mass in air at two different amplitudes. The force signal amplitude is normalized by the expected force amplitude.

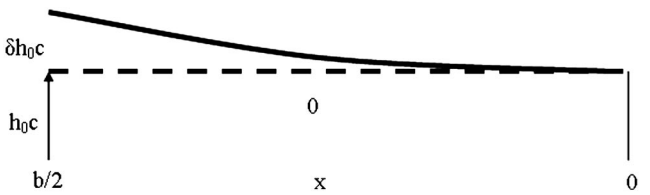

Fig. 4 Schematic drawing of a cantilevered plate, clamped at midspan, oscillated vertically at $h_0 c$ amplitude with the tip deflecting an extra $\delta h_0 c$.

III. Results

Figure 5 shows the registered force amplitude of a sinusoidal signal from varying the chordwise spacing of two plates, as well as the oscillation amplitude and frequency against, twice the theoretical value of the added mass for one plate. One can observe that, for the largest plate spacing of 0.5c, the registered force amplitude is independent of the spacing and oscillation amplitude and follows the linear theoretical prediction well. When decreasing the plate spacing to 0.25c, the curves start showing a larger slope, and thus a larger measured apparent mass. There is no dependency of normalized force on the oscillation amplitude until the plate spacing is decreased to 0.1c. Here, the increase in slope is exacerbated further and the oscillation amplitude of $h_0 = 0.05c$ deviates from the other curves. It is noted that the oscillation amplitude of $h_0 = 0.05c$ displaces the edge of the plate the same as the 0.1c edge-to-edge gap.

Fitting straight lines to the respective datasets in Fig. 5, the slopes of these lines are taken as the apparent mass. Figure 6 compares the measured apparent mass with Sedov's two-dimensional (2-D) calculation [13], for interplate gaps of 0.05c to 0.5c, with the zero gap taken as four times a single plate's apparent mass (and thus double that of two separate plates' apparent masses). The theory is invariant with oscillation amplitude, whereas the experiment considers 0.01c,

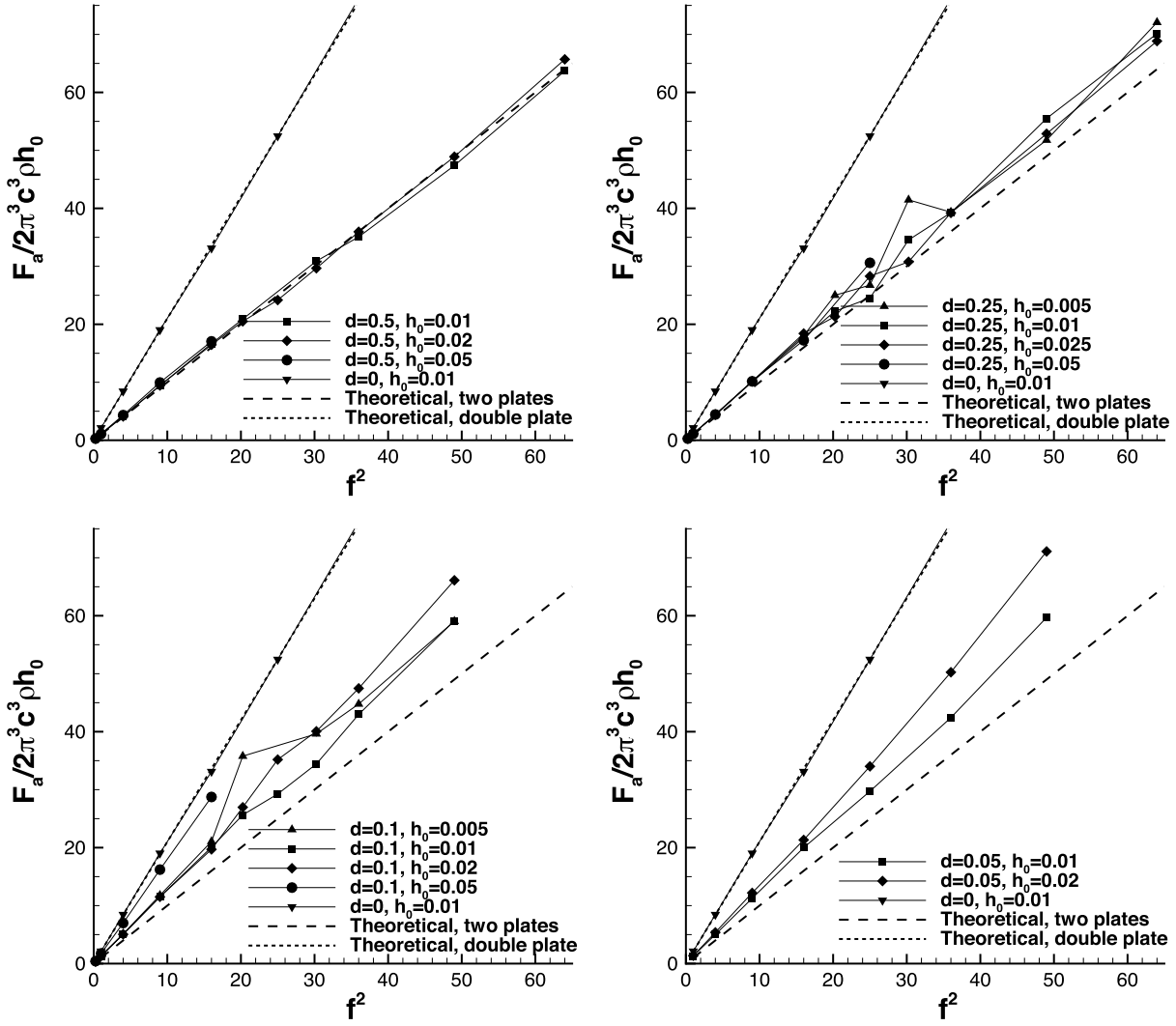

Fig. 5 Normalized sinusoidal force amplitude as a function of frequency squared with varying oscillation amplitude and varying plate spacing. Dashed curves are theoretical slopes 1 and 2 for two individual plates and two connected plates, respectively.

0.02c, and 0.05c amplitudes. Both the theory and experiment show an asymptotic relaxation from the zero gap to the small gap to (eventually) the infinite gap. The theory and experiment follow each other reasonably well, with some discrepancies that we note here. In the theory, the 0.5c interplate gap case exceeds the infinite-separation case by some 8%. In the experiment, this is also the case for the 0.005 oscillation amplitude; but, for smaller amplitudes, the 0.5c interplate gap has already attained the infinite-separation case. For all other interplate gaps, the highest oscillation amplitude examined here of 0.05c has the worst agreement with theory, especially at the smallest gaps (33% discrepancy for 0.05c amplitude and 0.1c gap). In the next section, we examine qualitatively how this small-gap disparity might be related to flowfield effects.

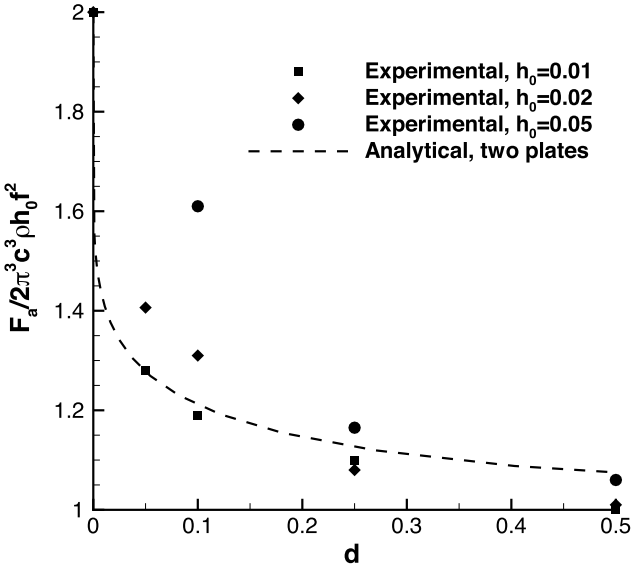

Fig. 6 Force amplitude for two plates with gap 'd' for three oscillation amplitudes compared to Sedov's theoretical solution [13].

IV. Flow Visualization

Figure 6 implies that, as the plate motion amplitude increases, the measured plate-normal force becomes progressively larger than that theoretically predicted from the apparent-mass contribution. If the entirety of the aerodynamic force is due to apparent mass, presumably, there are no discernible flowfield structures. We explore this qualitatively by examining the flowfield local to the gap between the plates and at the outboard edge of one of the plates. We look for 1) asymmetry in the flow patterns between upstroke and downstroke, 2) asymmetry between the inboard and outboard edges of the plate, and 3) whether the plates' motion produces a net outflow or whether dye deposition into the water around the plates' edges remains localized to the region of deposition. Where the upstroke flow pattern is symmetric with respect to that of the downstroke, and the dye streak remains localized to the injection point, we posit that circulatory effects are small compared to noncirculatory. Chordwise flow, from

Fig. 7 Flow visualization for $d = 0.05$, with $0.02c$ amplitude at 1 Hz oscillation. Gap dye injection (left) and one cycle later (middle) show vortex pairs producing a jet. Tip dye injection (right) shows vortex formation and flow entrainment towards the gap.

Fig. 8 5 Hz frequency, with $0.005c$ amplitude dye injected into the interplate gap: plate at extremum of upstroke (left), and at upstroke (right) five motion periods later.

Fig. 9 1 Hz oscillation, with $0.25c$ interplate gap and $0.02c$ oscillation amplitude, dye injected at interplate gap: upstroke extremum of plate motion (left); downstroke extremum, half-period later (middle), and another half-period later (right), back to upstroke extremum.

the plate outboard tip to the inboard, implies that the inter-plate gap is significant, in there being an asymmetry between outboard and inboard edges.

In Fig. 7, the two plates are $0.05c$ apart, oscillating at 1 Hz, with $0.02c$ amplitude. In the left and middle images of Fig. 7, dye is injected at the interplate gap. There is qualitative evidence of a vortex-pair shed at every semistroke, in opposition to the plate's motion (the pair convects downward on the upstroke, and vice versa). The resulting train of the vortex pairs produces, in the aggregate, a pair of jets normal to the plane of the plate. On the other hand, for a $0.005c$ stroke amplitude (Fig. 8), the plate-normal extent of this jet is quite muted, as each semistroke's vortex pair is entrained or "reingested" back toward the plate on the opposing semistroke, and successive strokes do not evince a train of vortex pairs or a jet. The localization of dye for the $0.005c$ amplitude but not the $0.02c$ amplitude suggests larger (though possibly still not large) circulatory effects for the latter, and it intuitively supports the larger deviation between the theory and experiment in Fig. 6 for larger oscillation amplitudes.

Dye injected at one of the plate's outboard edges (right-hand image in Fig. 7) does not move far into the plate-normal direction, in contradistinction to what happens in the intergap region. Instead, there is a slow convection from the outboard edge inboard toward the interplate gap. Upon reaching this gap, dye then forms the aforementioned jet. Thus, there is an asymmetry between the outboard and inboard (interplate gap) edges.

The situation in Fig. 9, also for a $0.02c$ amplitude at 1 Hz frequency, but now for a 0.25 interplate gap, is rather different. Now, there is no longer a jet or successive pairing of vortices emanating plate normal from the interplate gap, and evidence for flow along the plate from the outboard to the inboard edges is weak (if any). This suggests, first, that the $0.25c$ spacing is asymptoting to "infinity," which is consistent with the force data in Fig. 6; and second, that the circulatory effects are small. We conclude that the circulatory effects increase with an decreasing interplate gap and an increasing stroke amplitude.

V. Conclusions

The classical apparent-mass solution for a rigid flat plate, nominally in two dimensions, oscillating by a small amplitude in a direction normal to its surface is for a simply connected body. Consideration of two such bodies in close proximity was suggested as a problem probing the efficacy of superposition and small-disturbance theory. Accordingly, time-accurate direct force measurement in water of two harmonically oscillating coplanar neighboring rigid flat plates was compared with potential-flow theory. The plates were separated by a gap ranging from 0.05 to 0.5 chords, and they were oscillated at amplitudes of 0.005 to 0.05 chords.

The classical heuristic for a single-plate apparent mass is a circular cylinder of fluid with a diameter equal to the plate's chord. Two plates in direct contact along their edges therefore quadrupled the total apparent mass, whereas if the two plates were infinitely far apart, the total apparent mass would be merely double that of each plate. Sedov's 2-D potential flow model [13] was in agreement with experimental force measurement for the $0.005c$ amplitude; but, with higher oscillation amplitudes, the theory was less accurate. A plate separation of 0.5 chord produced an apparent mass close the infinite-separation case. Indeed, even for quarter- chord separation, the flow visualization shows that the time evolution of the intragap flow resembled that of the outboard plate edge, whereas for the 0.05 chord separation, each semistroke of the oscillation ejected a vortex pair in the average, producing a jet normal to the plates and resulting in a measured force larger than for the theoretical apparent mass.

Acknowledgments

This work was supported by the U.S. Air Force Office of Scientific Research Labtask 14RQ17COR, with Douglas Smith serving as Program Manager.

References

[1] Theodorsen, T., "General Theory of Aerodynamic Instability and the Mechanism of Flutter," NACA Rept. R-496, 1935.

[2] Küssner, H., "Untersuchung der Bewegung Einer Platte beim Eintritt in eine Strahlgrense," *Luftfahrtforschung*, Vol. 53, No. 12, 1936, pp. 229–425.

[3] von Karman, T., and Sears, W. R., "Airfoil Theory for Non-Uniform Motion," *Journal of the Aeronautical Sciences*, Vol. 5, No. 10, Aug. 1938, pp. 379–390. doi:10.2514/8.674

[4] Garrick, I. E., "On Some Reciprocal Relations in the Theory of Nonstationary Flows," NACA Rept. 629, 1938.

[5] Greenberg, J. M., "Airfoil in Sinusoidal Motion in a Pulsating Stream," NACA TR 1326, June 1947.

[6] Chow, C.-Y., and Huang, M.-K., "The Initial Lift and Drag of an Impulsively Started Airfoil of Finite Thickness," *Journal of Fluid Mechanics*, Vol. 118, May 1982, pp. 393–409. doi:10.1017/S002211208200113X

[7] Graham, J. M. R., "The Lift on an Aerofoil in Starting Flow," *Journal of Fluid Mechanics*, Vol. 133, Aug. 1983, pp. 413–425. doi:10.1017/S0022112083001986

[8] Pullin, D. I., and Wang, Z. J., "Unsteady Forces on an Accelerating Plate and Application to Hovering Insect Flight," *Journal of Fluid Mechanics*, Vol. 509, No. 1, 2004, pp. 1–21. doi:10.1017/S0022112004008821

[9] Ramesh, K. K., Gopalarathnam, A., Ol, M. V., Granlund, K. O., and Edwards, J., "Augmentation of Inviscid Airfoil Theory to Predict and Model 2-D Unsteady Vortex Dominated Flows," AIAA Paper 2011-3578, 2011.

[10] Granlund, K. O., Ol, M. V., and Bernal, L. P., "Unsteady Pitching Flat Plates," *Journal of Fluid Mechanics*, Vol. 733, Oct. 2013, Paper R5. doi:10.1017/jfm.2013.444

[11] Pitt-Ford, C. W., and Babinsky, H., "Lift and the Leading-Edge Vortex," *Journal of Fluid Mechanics*, Vol. 720, April 2013, pp. 280–313. doi:10.1017/jfm.2013.28

[12] Yu, H.-T., Bernal, L. P., Granlund, K. O., and Ol, M. V., "Aerodynamics of Pitching Wings: Theory and Experiments," AIAA Paper 2014-2881, 2014.

[13] Sedov, L. I., *Two-Dimensional Problems in Hydrodynamics and Aerodynamics*, Wiley, New York, 1965, pp. 58–61.

[14] Brennen, C. E., "A Review of Added Mass and Fluid Inertial Forces," Naval Civil Engineering Lab. TR CR-82.010, Port Hueneme, CA, Jan. 1982.

E. Gutmark
Associate Editor